Molecular Interaction of Poly(acrylic acid) Gold Nanoparticles with Human Fibrinogen

Zhou J. Deng,[†] Mingtao Liang,[‡] Istvan Toth,[‡] Michael J. Monteiro,[§] and Rodney F. Minchin[†,*]

[†]School of Biomedical Sciences, [‡]School of Chemistry and Molecular Biosciences, and [§]Australian Institute for Bioengineering and Nanotechnology, University of Queensland, Brisbane, Australia

ABSTRACT

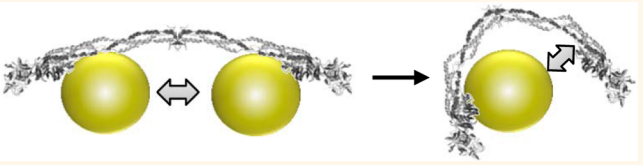

The binding of fibrinogen to various nanoparticles can result in protein unfolding and exposure of cryptic epitopes that subsequently interact with cell surface receptors. This response is dependent on the size, charge, and concentration of the nanoparticle. Here we examine the binding kinetics of human fibrinogen to negatively charged poly(acrylic acid)-coated gold nanoparticles ranging in size from 7 to 22 nm. These particles have previously been shown to elicit an inflammatory response in human cells. The larger nanoparticles bound fibrinogen with increasing affinity and a slower dissociation rate. Each fibrinogen molecule could accommodate two 7 nm nanoparticles but only one when the diameter increased to 10 nm. Nanoparticles larger than 12 nm bound multiple fibrinogen molecules in a positively cooperative manner. However, in the presence of excess nanoparticle, fibrinogen induced aggregation of the larger particles that could bind more than one protein molecule. This is consistent with interparticle bridging by the fibrinogen. Taken together, these results demonstrate that subtle changes in nanoparticle size can influence protein binding both with the surface of the nanoparticle and within the protein corona.

KEYWORDS: fibrinogen · poly(acrylic acid) · gold · interaction · kinetics · configuration

The binding of proteins to nanoparticles in physiological fluids, such as plasma, can influence the biological properties of the nanoparticles.[1−3] Surface-bound proteins can promote cell-specific uptake,[4,5] as well as activation of intracellular signaling pathways.[6] Most nanoparticles bind to an array of proteins forming both a "soft" corona of weakly bound proteins and a "hard" corona of tightly bound proteins.[7] While surface proteins can influence the physical properties of the nanoparticles, the nanoparticles can also influence the structural characteristics of the protein. Changes in protein conformation and protein unfolding may expose amino acid sequences that are normally buried within the folded protein.[8] These cryptic epitopes can often interact with cell surface receptors and influence tissue uptake, biodistribution, and receptor activation once nanoparticles enter the circulation.

Fibrinogen has been reported to bind to a wide range of nanoparticles, including metal oxides,[9] carbon black,[10] polymeric nanoparticles,[11] and single-walled carbon nanotubes.[12] The heterogeneity of these particles suggests that fibrinogen contains a number of different binding domains that accommodate the different nanoparticles. Fibrinogen is a large cylindrical molecule with a length of approximately 45 nm.[13] It is a centrosymmetric protein of two halves, each comprising three polypeptides. Previously, we reported that poly(acrylic acid) polymer-coated gold nanoparticles (PAA-GNP) selectively interact with fibrinogen in human plasma.[6] The hard corona that formed when these particles were exposed to plasma almost exclusively comprised the three chains of fibrinogen. Upon binding, protein unfolding exposed a cryptic peptide located in the C-terminus of the fibrinogen γ-chain that specifically interacted with Mac-1 receptors, resulting in NF-κB-dependent cytokine release from human monocytic cells. This pro-inflammatory effect was most evident with small particles (5−10 nm) and was only seen with larger particles (*ca.* 20 nm) when nonsaturating protein binding was examined. The previous study illustrated that relatively small changes in nanoparticle diameter could affect protein binding in addition to biological responses. However, the molecular mechanism and binding kinetics of nanoparticles and fibrinogen remain to be elucidated.

A major advantage of polymer-coated gold nanoparticles is their ease of preparation with

* Address correspondence to r.minchin@uq.edu.au.

Received for review July 5, 2012 and accepted September 20, 2012.

Published online September 20, 2012
10.1021/nn3029953

TABLE 1. Characterization of the PAA-GNPs

nanoparticle (PAA-GNP)	diameter of gold core (nm)	diameter after polymer coating (nm)	ζ-potential (mV)	polydispersity index
7 nm	5.7 ± 0.07	7.1 ± 0.06	−25.2 ± 3.5	0.11
10 nm	8.5 ± 0.09	10.0 ± 0.15	−37.4 ± 0.9	0.09
12 nm	10.8 ± 0.33	11.9 ± 0.35	−36.9 ± 6.6	0.08
15 nm	13.4 ± 0.18	14.5 ± 0.63	−39.6 ± 0.2	0.06
17 nm	15.6 ± 0.16	17.6 ± 0.28	−41.1 ± 4.9	0.09
19 nm	17.0 ± 0.27	18.9 ± 0.20	−45.1 ± 3.6	0.08
22 nm	20.8 ± 0.40	21.8 ± 0.80	−49.9 ± 4.1	0.04

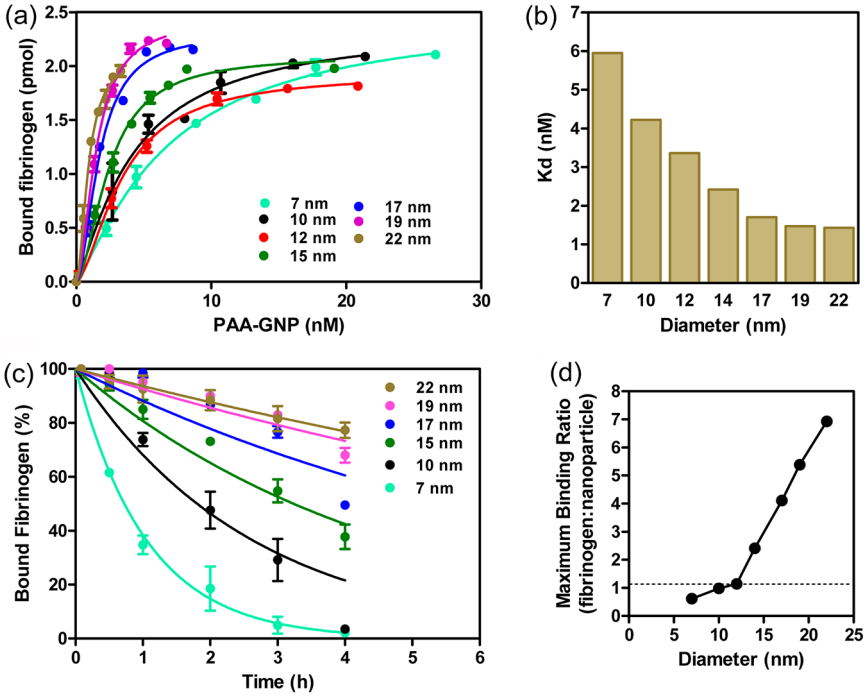

Figure 1. (a) Concentration-dependent binding of fibrinogen to different sized PAA-GNPs. Results are mean ± SEM, n = 3. (b) Effect of nanoparticle diameter on the equilibrium binding constant (K_d) of fibrinogen. K_d values were estimated by fitting eq 1 to the data in a. (c) Dissociation of fibrinogen from PAA-GNP in the presence of excess unlabeled fibrinogen. On the basis of the law of mass action, an exponential curve was fitted to each data set (solid lines) and was used to estimate the dissociation rate constants for each nanoparticle. For the 10 nm particles, the 4 h time point was omitted from the analysis as it did not follow an exponential decay. Results are mean ± SEM, n = 3. (d) Effect of nanoparticle diameter on the number of fibrinogen molecules bound. Maximum binding ratio was determined from the data shown in a.

a narrow diameter range.[14] Moreover, polymers can be grafted to the gold surface at high densities (*ca.* 1 chain/nm^2). Under these conditions, the polymers adopt a brush-like configuration and protein interaction occurs primarily with the terminal groups of the polymer chains. Here, to better understand the size-dependent binding of nanoparticles to fibrinogen, a series of PAA-GNP was synthesized, as previously reported,[14] and used to characterize their molecular interactions with human fibrinogen.

RESULTS AND DISCUSSION

The PAA-GNPs ranged in diameter from 5.7 to 21.8 nm, as determined by dynamic light scattering, and were monodispersed in solution, as shown by their low polydispersity indices (Table 1). Moreover, the ζ-potential for each PAA-GNP showed that they were highly negatively charged. Each of the PAA-GNP bound to fibrinogen with saturating kinetics (Figure 1a). The binding curves shifted to the left with an increase in PAA-GNP size indicative of increased binding affinity. To determine the binding kinetics for each of the nanoparticles, the Hill equation was fitted to the data by nonlinear least-squares regression. The dissociation constant K_d decreased progressively from approximately 6 nM for the smallest nanoparticles to less than 1.5 nM for the largest nanoparticles (Figure 1b). The change in free energy, estimated using the Gibbs equation, ranged from 48.8 to 52.5 kJ/mol, indicative of high affinity binding similar to that seen with antigen−antibody interactions.[15] The decrease in K_d with increasing diameter suggests an increase in the number of molecular interactions between the protein and the nanoparticles as surface area increased. Under

TABLE 2. Kinetic Parameters for Fibrinogen Binding to PAA-GNPs

nanoparticle (PAA-GNP)	k_{on} (nM^{-1} h^{-1})	k_{off} (h^{-1})	Hill coefficient (h)
7 nm	0.16	0.97 ± 0.03	1.14 ± 0.28
10 nm	0.09	0.38 ± 0.03	1.24 ± 0.42
12 nm	ND[a]	ND[a]	1.61 ± 0.30
15 nm	0.09	0.21 ± 0.02	1.73 ± 0.16
17 nm	0.07	0.12 ± 0.02	1.79 ± 0.19
19 nm	0.05	0.08 ± 0.01	1.78 ± 0.14
22 nm	0.04	0.06 ± 0.01	1.84 ± 0.29

[a] ND = not determined.

these conditions of excess fibrinogen, no aggregation of the nanoparticles was observed (see below).

The rate of dissociation was measured by incubating fluorescently labeled fibrinogen bound to each nanoparticle with excess (100-fold) unlabeled fibrinogen. The appearance of fluorescence in the medium with time was assessed after centrifugation. Figure 1c illustrates the loss of surface-bound fluorescently labeled protein over 4 h. As the size of the nanoparticles increased, the rate of dissociation decreased, which further suggests greater molecular interaction between the fibrinogen and the larger nanoparticles. In the absence of excess protein, no desorption of fibrinogen from any of the nanoparticles was observed (Supporting Information). This is most likely due to rapid reabsorption when no competing protein is present in the medium. The dissociation rate constant (k_{off}) was estimated by fitting an exponential decay curve to the data. As the size of the PAA-GNP increased, k_{off} decreased from almost 1 h^{-1} to less than 0.1 h^{-1} (Table 2). The association rate constant (k_{on}), calculated as the ratio of k_{off} to K_d, was essentially independent of nanoparticle size, except for the 7 nM PAA-GNP where k_{on} was approximately 2-fold higher. A possible explanation for this is provided below where the binding stoichiometry is discussed.

The Hill coefficient (h) measures the degree of independence for interaction between multiple binding sites. For the two smallest PAA-GNPs, h was not different to 1 (Table 2), indicating that the binding of fibrinogen to these nanoparticles involved a single binding site or multiple sites that were independent of one another. By contrast, when the diameter of the PAA-GNP exceeded 10 nm, h was significantly greater than 1, indicating the presence of multiple binding sites that are dependent on one another. Interestingly, the binding of fibrinogen to citrate-coated gold nanoparticles within the same size range as those used in the current study showed quite different kinetics.[16] Significant negative cooperativity was observed with Hill coefficients less than 1 for nanoparticles larger than 5 nm diameter. However, the apparent binding affinity increased similar to that reported here, which supports the notion that nanoparticles of different diameters

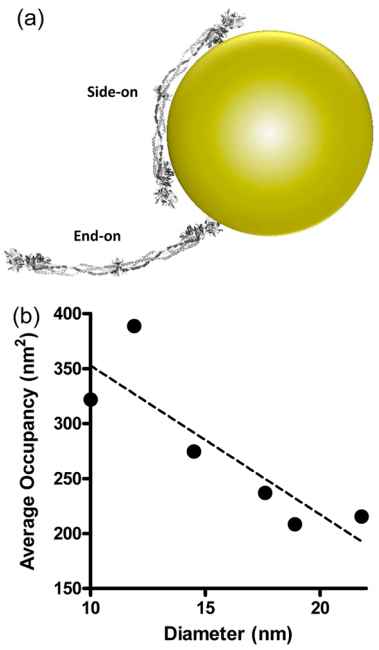

Figure 2. (a) Model illustrating the side-on *versus* end-on configurations for the binding of fibrinogen to the surface of a nanoparticle. (b) Plot of the average occupancy of fibrinogen on the different PAA-GNPs. Average occupancy was calculated based on the surface area of the nanoparticle and the average number of bound fibrinogen per nanoparticle.

interact with fibrinogen differently. We have also previously reported that gold nanoparticles decorated with positively charged polymers still bind to fibrinogen with high affinity but do not unfold the protein to elicit an inflammatory response as was seen with the PAA-GNP.[17] Taken together, these studies suggest that fibrinogen can interact with an array of nanoparticles with varying surface characteristics, but the binding kinetics and biological outcomes may be very different.

At maximum binding capacity, the stoichiometry between the bound fibrinogen and the nanoparticles was dependent on particle size (Figure 1d). For the 7 nm PAA-GNP, maximum binding occurred at approximately 1 fibrinogen per 2 nanoparticles, which is consistent with the multiple independent binding sites suggested by $h = 1$. For the 10 and 12 nm PAA-GNPs, maximum binding occurred at 1:1 stoichiometry. By contrast, PAA-GNPs larger than 12 nm bound multiple fibrinogen molecules, increasing linearly with the size of the nanoparticle. Nonspheroid or fibrous proteins, such as fibrinogen, can interact with a surface in a number of configurations (Figure 2a). Both side-on and end-on binding of fibrinogen to different substrates have been described.[18,19] The side-on cross-sectional area of fibrinogen is 128 nm^2, while the end-on cross-sectional area is only 35.3 nm^2.[18] On the basis of the number of fibrinogen proteins bound to each of the PAA-GNP, it is possible to calculate the average surface area occupied by each protein molecule. For the 10 and 12 nm particles, the occupied area was 321 and

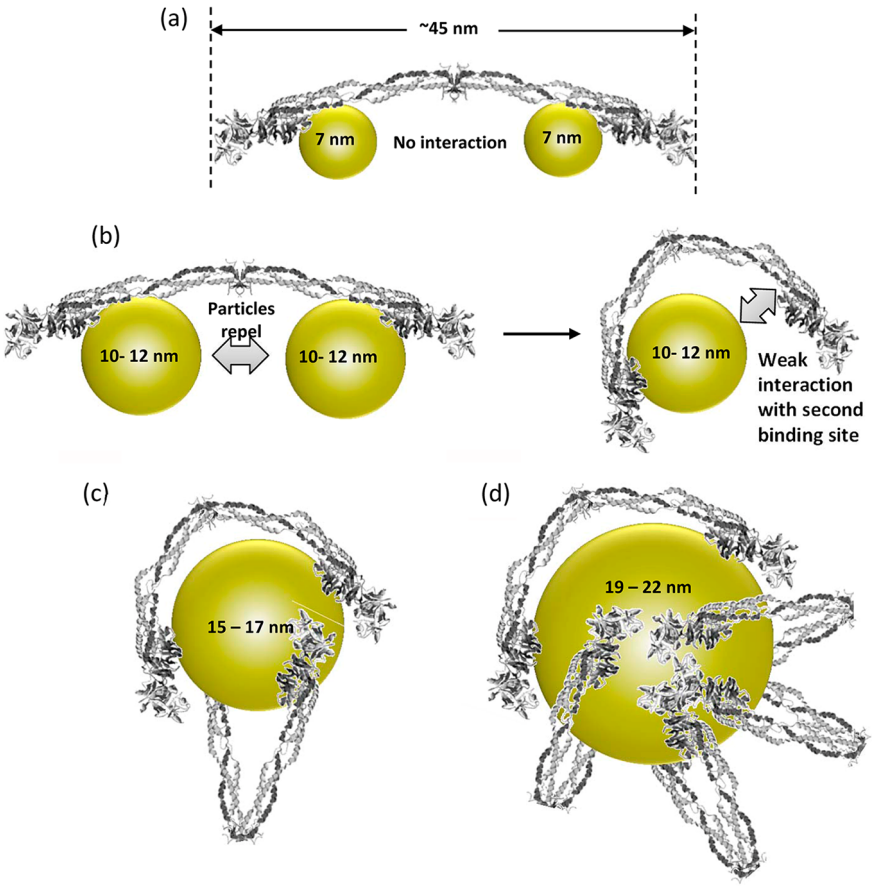

Figure 3. (a) Binding of small (7 nm) PAA-GNPs to fibrinogen showing two nanoparticles bound to each protein molecule. (b) Larger sized nanoparticles inhibit the binding of two particles to each fibrinogen. As the diameter of the nanoparticle increases, the second binding site can come into contact with the nanoparticle due to flexibility at the E-domain of the protein. (c,d) Larger nanoparticles can accommodate multiple fibrinogen molecules due to the larger surface area.

388 nm^2, respectively. Because the binding ratio for these nanoparticles was 1:1, the apparent increase in occupancy was due to the increase in the nanoparticle surface area. At greater diameters, the area occupied by each fibrinogen molecule decreased with size, indicating a more tightly packed configuration on the surface of the larger particles (Figure 2b). These data are in agreement with the side-on binding configuration. Roach *et al.* found that fibrinogen bound to silica nanoparticles of 15−60 nm in diameter *via* a side-on configuration, in which the protein wraps around the nanoparticle to minimize the free surface energy.[20] The larger PAA-GNPs also demonstrated positive cooperativity with fibrinogen interaction ($h > 1$), indicating that the binding of one protein molecule was able to facilitate the binding of further protein molecules to the nanoparticle surface. Both PAA-GNP and fibrinogen have a net negative charge, potentially reducing the overall negative nanoparticle surface charge with the bound protein providing a shielding effect. This shielding consequently reduced the nonspecific electrostatic repulsion between the surface and the protein in solution, enhancing the binding of subsequent fibrinogen molecules.

The different binding behaviors of the various PAA-GNPs can be explained by the increase in their surface areas. The smallest nanoparticles can bind to the two fibrinogen sites independent of one another, as illustrated in Figure 3a. It has been proposed that these two sites are located at the C-termini of the α-chains, which are cationic under physiological conditions[6] (Figure 3a). As these are independent events, there is a higher probability of protein−nanoparticle interaction, which is reflected in the greater association rate constant. As the size of the PAA-GNPs increased to 10−12 nm, there was a transition from one-site binding to two-site binding. The increase in diameter will increase the presence of Coulombic repulsion between the bound nanoparticles. This results in a maximum 1:1 binding ratio for the 10−12 nm PAA-GNPs (Figure 3b). Fibrinogen is commonly presented as a linear cylindrical molecule.[21,22] However, several studies have shown that it is relatively flexible around the central E-domain.[23,24] Using electron microscopy, Beilbom *et al.* observed that the average angle of bend (θ) at the E-domain was 22°.[23] While most molecules exhibited a θ value of 0−5°, some could bend as much as 90°. This flexibility suggests that both binding sites on

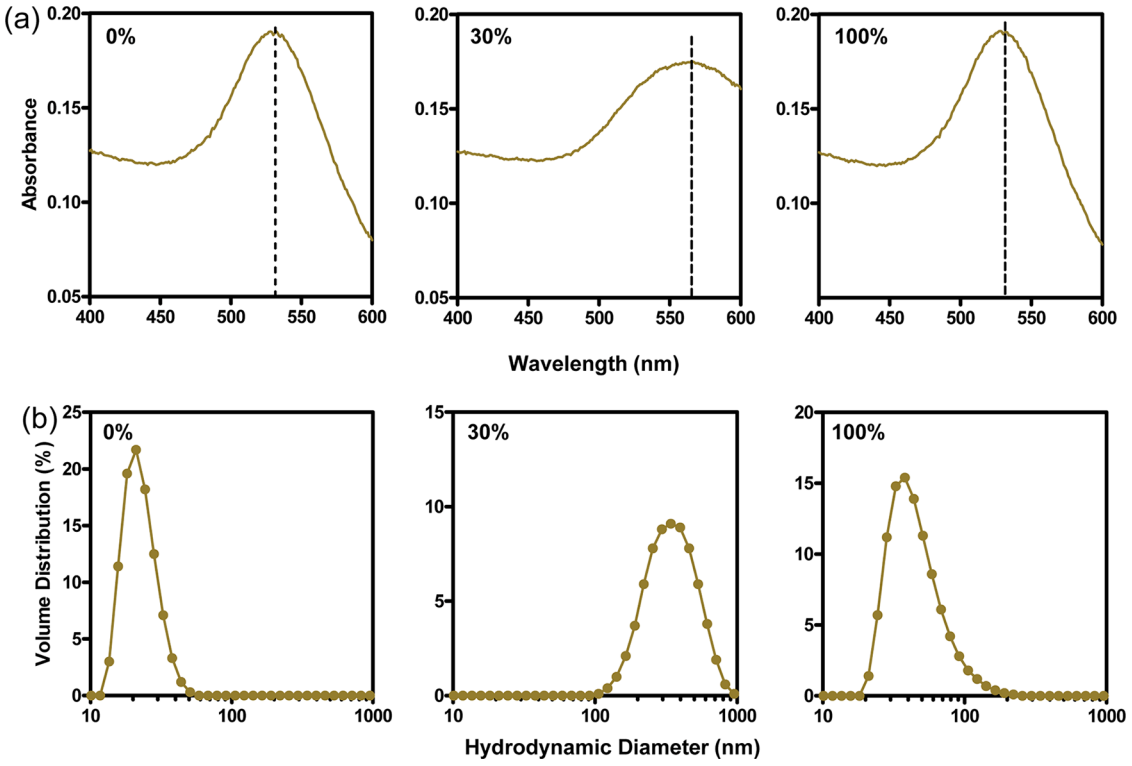

Figure 4. (a) Shift in the 22 nm PAA-GNP absorption spectra following binding of fibrinogen. In the absence of protein (left panel), absorption maximum is 528 nm. At 30% maximum binding capacity, the absorption peak shifted to 570 nm (middle panel). At maximum binding capacity, the absorption spectrum was similar to nanoparticles alone (right panel). (b) Hydrodynamic diameters of the 22 nm PAA-GNP in the presence of fibrinogen at 0, 30, and 100% maximum binding capacity.

the fibrinogen can interact with a single nanoparticle of sufficient diameter (Figure 3c). As fibrinogen binds more tightly *via* the two-site binding, affinity increased and the rate of dissociation decreased. For PAA-GNPs larger than 12 nm, multiple protein molecules could bind, as illustrated in Figure 3d, leading to a highly packed fibrinogen corona, as indicated by the decrease in surface occupancies (Figure 2b). It is speculated that this crowding effect at maximum binding capacity sterically hinders access of the Mac-1 binding sequence to its receptor, providing a possible explanation for the inability of the 20 nm PAA-GNPs to induce cytokine release.[6]

All of the above studies were performed in the presence of excess fibrinogen. However, when the binding of the protein to PAA-GNP was examined in the presence of excess nanoparticle, rapid aggregation was observed for nanoparticles larger than 12 nm, as measured by surface plasmon resonance spectroscopy (Figure 4). For the 22 nm PAA-GNP, the absorption spectra shifted to longer wavelengths at 30% maximum binding capacity (Figure 4a), indicating clustering of the nanoparticles.[25] However, at 100% maximum binding capacity, the absorption spectrum was similar to that for PAA-GNP in the absence of fibrinogen, suggesting no aggregation of the nanoparticles under these conditions. Particle aggregation was independently confirmed by dynamic light scattering studies (Figure 4b). The nanoparticles alone exhibited a mean diameter of approximately 21 nm, which increased to 450 nm at 30% maximum binding capacity. By contrast, at 100% maximum binding capacity, the particle size was only 38 nm, which represented the PAA-GNP plus the protein corona of 7−8 nm thickness.[6]

The red shift of the absorption spectra was only seen for the PAA-GNP larger than 12 nm in diameter (Figure 5a). Thus, aggregation was only seen for those large nanoparticles that were able to bind multiple fibrinogen molecules. Moreover, this was not seen when fibrinogen was replaced by albumin (Figure 5b), which binds poorly to PAA-GNP.[6] Finally, digestion of the fibrinogen with plasmin prevented PAA-GNP aggregation, indicating that the intact structure of fibrinogen was essential for this effect. The enzymatic degradation of the fibrinogen was confirmed by SDS-PAGE (Figure 5c). These results suggest that the intraparticle and interparticle binding of fibrinogen is dependent on both the size and concentration of the nanoparticles. When PAA-GNPs were in excess, the interaction favored the binding of one fibrinogen protein to multiple nanoparticles if the nanoparticle had the capacity to bind more than one molecule of the protein. In this case, fibrinogen probably bridges the nanoparticles *via* a dumbbell-like configuration and facilitates the agglomeration process. By contrast, when fibrinogen was in excess, the rapid formation of

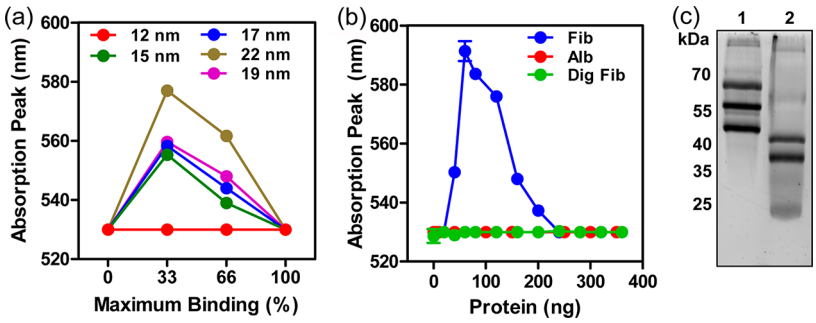

Figure 5. (a) Change in absorption peak for the different sized nanoparticles with respect to binding saturation. (b) Effect of fibrinogen (Fib), albumin (Alb), and plasmin-digested fibrinogen (Dig Fib) on the absorption peak for 22 nm PAA-GNPs. (c) SDS-PAGE gel of fibrinogen (lane 1) and plasmin-digested fibrinogen (lane 2).

a tightly packed corona prevented interparticle binding, and aggregation was not seen.

It has been reported that fibrinogen is able to induce the aggregation of various nanoparticles including silica, carbon black, and surface-modified polystyrene nanoparticles.[10] The morphology of the aggregates, as measured by scanning electron microscopy, indicated bridging effects of fibrinogen on these nanoparticles. Other large, elongated molecules, such as polymers or DNA, can also induce aggregation of the gold nanoparticles.[26] Nanoparticle aggregation *in vivo* is associated with increased clearance rates,[27] which has implications for determining the accurate doses of surface exposure to cells and tissues.[10]

Because proteins in the corona can both enhance and inhibit biological responses to nanoparticles, it is important to understand the molecular events that determine high affinity, long-lived protein–nanoparticle interactions compared to low affinity, rapidly exchanging interactions. It has been proposed that proteins bound tightly in the corona might provide a map of the pathway that a particle travels as it traverses various biological compartments.[28] If this is the case, then the protein corona, in particular, the most tightly bound proteins, will provide important information about the fate of nanoparticles *in vivo*. As a greater understanding of protein–nanoparticle interactions emerges, particle design may be modified to take advantage of protein binding in order to modulate biodistribution *in vivo*. This has previously been demonstrated with apolipoprotein E-mediated delivery of poly(butyl cyanoacrylate) nanoparticles across the blood–brain barrier.[29] Alternatively, modification of nanoparticles to avoid certain protein binding that contributes to adverse effects may eventually add to the safer development of therapeutically useful nanoparticles for drug delivery, medical imaging, and diagnosis.

Protein unfolding as a consequence of binding to the surface of nanoparticles has been widely reported.[2,6,30,31] This can lead to protein aggregation or the unmasking of cryptic epitopes that bind to specific cellular receptors. Indeed, by studying nanoparticle–protein interactions, it is feasible that new biological functions for different proteins may be revealed as cryptic epitopes are identified.

CONCLUSION

We have examined the molecular interaction between fibrinogen and PAA-GNP of increasing sizes from 7 to 22 nm in diameter. On the basis of the experimental data, it is proposed that the nanoparticle–fibrinogen interaction can have distinct binding configuration and affinities depending on the size of the nanoparticles. The results also support a two binding sites model for PAA-GNP interaction with fibrinogen. Importantly, this study demonstrates how subtle changes in nanoparticle size can markedly influence nanoparticle–protein interactions and aggregation. It also emphasizes the importance of understanding the dynamics of nanoparticle–protein interactions because changes in these interactions can affect biological outcomes.

METHODS

Nanoparticles. Polymer–gold nanoparticles were synthesized and characterized as reported elsewhere.[14]

Fibrinogen Labeling. Alexa Fluor 647 succinimidyl ester (Invitrogen) reconstituted in dimethyl sulfoxide was used to fluorescently label the fibrinogen protein in 150 mM sodium bicarbonate, pH 8.5. A far-red fluorescent dye was chosen to minimize interference from the gold nanoparticles. The concentrations of fibrinogen and dye were 2.5 mg/mL and 125 μg/mL, respectively. After 1 h incubation at room temperature, free dye was removed using a PD-10 desalting column (GE health) in phosphate buffered saline (PBS, 150 mM NaCl, 10 mM phosphate, pH 7.4). The concentrations of labeled fibrinogen were determined by the absorbance at 280 nm using a spectrophotometer (NanoDrop, Thermo Scientific). The ratio of dye to fibrinogen was approximately 7:1. This represented a molar ratio of 1:60 for dye/positively charged amino acid in fibrinogen. The samples were stored in aliquots at −20 °C until used.

Binding Studies. For the protein pull-down studies, 1 μg of fluorescently labeled fibrinogen in 100 μL of PBS was incubated

with increasing amount of the nanoparticles. The incubation was carried out at 37 °C for 5 min followed by centrifugation at 50 000*g* for 30 min. The amount of fibrinogen in the supernatant was then determined by fluorescent spectroscopy (POLARstar, BMG Labtech). Protein-only controls showed that no fibrinogen pelleted under the centrifugation conditions. All experiments were performed in triplicate.

A trace level of background fluorescence in the supernatants was seen during the pull-down experiments, which was due to residual dye after desalting the samples. This background signal was subtracted from all of the fluorescence measurements when calculating the fibrinogen amounts. Nonspecific adsorption of fibrinogen to the tubes during the incubation was determined using a fibrinogen-only control. On the basis of the control experiments, the free fibrinogen was approximately 0.7 μg (*i.e.*, 7 μg/mL), which was taken into account to calculate the total amount of available fibrinogen. After centrifugation, the amount of nanoparticle-bound fibrinogen was calculated by subtracting the amount of fibrinogen measured in the supernatant from the total fibrinogen.

The amount of bound fibrinogen (pmol) was plotted against the concentration of the PAA-GNPs (nM). The molarity of the PAA-GNPs and fibrinogen was determined using the nanoparticle density of 19.3 g/cm^3 and fibrinogen molecular weight of 340 kDa. A binding saturation curve was fitted to the protein pull-down data. The binding affinities and maximal binding capacity were determined by nonlinear least-squares regression analysis (Prism 5, GraphPad Software) using the equation

$$B = \frac{B_{max}[NP]^h}{K_d{}^h + [NP]^h} \quad (1)$$

where B is bound fibrinogen, B_{max} is the maximum binding capacity, [NP] is the concentration of PAA-GNP, K_d is equilibrium binding constant, and h is the Hill coefficient.

For the competition assay, a slight excess amount of each nanoparticle (7 nm = 17.7 nM; 10 nm = 16 nM; 15 nm = 8.2 nM; 17 nm = 5.2 nM; 19 nm = 4 nM; 22 nm = 3.3 nM) was incubated with 1 μg of fluorescently labeled fibrinogen at 37 °C for 5 min. After the initial incubation, 100-fold excess unlabeled fibrinogen was added and incubated at 37 °C for up to 240 min. At different time points, individual samples were centrifuged, and the amount of the labeled fibrinogen in the supernatants was determined as described above. Separate samples were used at each time point. A one-phase exponential decay curve was used to model the dissociation of the fibrinogen from the nanoparticle surface. The dissociation rate constants, K_{off}, of the protein–nanoparticle complexes were determined by fitting the equation to the data:

$$Y = 100e^{-K_{off}t} \quad (2)$$

where Y is the bound fibrinogen (% total), t is time (min), and K_{off} is the dissociation rate constant (min^{-1}). All of the experiments were performed in triplicate.

Spectroscopic Study of PAA-GNP Aggregation. To examine the aggregation of the PAA-GNPs in the presence of fibrinogen, the nanoparticles (35 μg/mL) were incubated with fibrinogen at 37 °C for 5 min. The amount of fibrinogen used was equivalent to 0, 30, 60, and 100% of the maximum binding capacity. After incubation, 100 μL of each sample was used to determine the absorption spectra (POLARstar, BMG Labtech). The surface plasmon resonance (SPR) peaks of the PAA-GNP colloid were determined by the position of the maximal absorbance peak between 520 and 600 nm.[2,3] The experiments were performed in triplicate.

To prepare plasmin-digested fibrinogen, fibrinogen at a concentration of 0.4 mg/mL was incubated with 0.006 mg/mL (≥0.012 units/mL) plasmin (Sigma-Aldrich) at 37 °C for 60 min.[4] After the incubation, the digestion was stopped by heating the sample at 56 °C for 5 min. The digested fibrinogen samples were stored in aliquots at −20 °C until used.

Conflict of Interest: The authors declare no competing financial interest.

Acknowledgment. This work was supported by grants from the Australian Research Council (Grant No. DP0878733) and the National Health and Medical Research Council (Grant No. 569694).

Supporting Information Available: Additional experimental details. This material is available free of charge *via* the Internet at http://pubs.acs.org.

REFERENCES AND NOTES

1. Lynch, I.; Dawson, K. A. Protein–Nanoparticle Interactions. *Nano Today* **2008**, *3*, 40–47.
2. Nel, A. E.; Madler, L.; Velegol, D.; Xia, T.; Hoek, E. M. V.; Somasundaran, P.; Klaessig, F.; Castranova, V.; Thompson, M. Understanding Biophysicochemical Interactions at the Nano-Bio Interface. *Nat. Mater.* **2009**, *8*, 543–557.
3. Oberdorster, G. Safety Assessment for Nanotechnology and Nanomedicine: Concepts of Nanotoxicology. *J. Intern. Med.* **2010**, *267*, 89–105.
4. Chithrani, B. D.; Chan, W. C. W. Elucidating the Mechanism of Cellular Uptake and Removal of Protein-Coated Gold Nanoparticles of Different Sizes and Shapes. *Nano Lett.* **2007**, *7*, 1542–1550.
5. Lesniak, A.; Campbell, A.; Monopoli, M. P.; Lynch, I.; Salvati, A.; Dawson, K. A. Serum Heat Inactivation Affects Protein Corona Composition and Nanoparticle Uptake. *Biomaterials* **2010**, *31*, 9511–9518.
6. Deng, Z. J.; Liang, M.; Monteiro, M.; Toth, I.; Minchin, R. F. Nanoparticle-Induced Unfolding of Fibrinogen Promotes Mac-1 Receptor Activation and Inflammation. *Nat. Nanotechnol.* **2011**, *6*, 39–44.
7. Casals, E.; Pfaller, T.; Duschl, A.; Oostingh, G. J.; Puntes, V. Time Evolution of the Nanoparticle Protein Corona. *ACS Nano* **2010**, *4*, 3623–3632.
8. Lynch, I. Are There Generic Mechanisms Governing Interactions between Nanoparticles and Cells? Epitope Mapping the Outer Layer of the Protein–Material Interface. *Physica A* **2007**, *373*, 511–520.
9. Deng, Z. J.; Mortimer, G.; Schiller, T.; Musumeci, A.; Martin, D.; Minchin, R. F. Differential Plasma Protein Binding to Metal Oxide Nanoparticles. *Nanotechnology* **2009**, *20*, 455101.
10. Kendall, M.; Ding, P.; Kendall, K. Particle and Nanoparticle Interactions with Fibrinogen: The Importance of Aggregation in Nanotoxicology. *Nanotoxicology* **2011**, *5*, 55–65.
11. Cedervall, T.; Lynch, I.; Lindman, S.; Berggard, T.; Thulin, E.; Nilsson, H.; Dawson, K. A.; Linse, S. Understanding the Nanoparticle–Protein Corona Using Methods To Quantify Exchange Rates and Affinities of Proteins for Nanoparticles. *Proc. Natl. Acad. Sci. U.S.A.* **2007**, *104*, 2050–2055.
12. Song, L.; Meng, J.; Zhong, J.; Liu, L.; Dou, X.; Liu, D.; Zhao, X.; Luo, S.; Zhang, Z.; Xiang, Y.; *et al.* Human Fibrinogen Adsorption onto Single-Walled Carbon Nanotube Films. *Colloids Surf., B* **2006**, *49*, 66–70.
13. Vauthier, C.; Persson, B.; Lindner, P.; Cabane, B. Protein Adsorption and Complement Activation for Di-block Copolymer Nanoparticles. *Biomaterials* **2011**, *32*, 1646–1656.
14. Liang, M.; Lin, I. C.; Whittaker, M. R.; Minchin, R. F.; Monteiro, M. J.; Toth, I. Cellular Uptake of Densely Packed Polymer Coatings on Gold Nanoparticles. *ACS Nano* **2010**, *4*, 403–413.
15. Kastritis, P. L.; Moal, I. H.; Hwang, H.; Weng, Z.; Bates, P. A.; Bonvin, A. M.; Janin, J. A Structure-Based Benchmark for Protein–Protein Binding Affinity. *Protein Sci.* **2011**, *20*, 482–491.
16. Lacerda, S. H.; Park, J. J.; Meuse, C.; Pristinski, D.; Becker, M. L.; Karim, A.; Douglas, J. F. Interaction of Gold Nanoparticles with Common Human Blood Proteins. *ACS Nano* **2010**, *4*, 365–379.
17. Deng, Z. J.; Liang, M.; Toth, I.; Monteiro, M.; Minchin, R. F. Plasma Protein Binding of Positively and Negatively Charged Polymer-Coated Gold Nanoparticles Elicits Different Biological Responses. *Nanotoxicology* **2012**, 10.3109/17435390.2012.655342.
18. Adamczyk, Z.; Barbasz, J.; Ciesla, M. Mechanisms of Fibrinogen Adsorption at Solid Substrates. *Langmuir* **2011**, *27*, 6868–6878.

19. Riedel, T.; Suttnar, J.; Brynda, E.; Houska, M.; Medved, L.; Dyr, J. E. Fibrinopeptides A and B Release in the Process of Surface Fibrin Formation. *Blood* **2011**, *117*, 1700–1706.
20. Roach, P.; Farrar, D.; Perry, C. C. Surface Tailoring for Controlled Protein Adsorption: Effect of Topography at the Nanometer Scale and Chemistry. *J. Am. Chem. Soc.* **2006**, *128*, 3939–3945.
21. Brown, J. H.; Volkmann, N.; Jun, G.; Henschen-Edman, A. H.; Cohen, C. The Crystal Structure of Modified Bovine Fibrinogen. *Proc. Natl. Acad. Sci. U.S.A.* **2000**, *97*, 85–90.
22. Kollman, J. M.; Pandi, L.; Sawaya, M. R.; Riley, M.; Doolittle, R. F. Crystal Structure of Human Fibrinogen. *Biochemistry* **2009**, *48*, 3877–3886.
23. Beijbom, L.; Larsson, U.; Kaveus, U.; Hebert, H. Structure Analysis of Fibrinogen by Electron Microscopy and Image Processing. *J. Ultrastruct. Mol. Struct. Res.* **1988**, *98*, 312–319.
24. Apap-Bologna, A.; Webster, A.; Raitt, F.; Kemp, G. The Influence of Calcium Ions on Fibrinogen Conformation. *Biochim. Biophys. Acta* **1989**, *995*, 70–74.
25. Guarise, C.; Pasquato, L.; Scrimin, P. Reversible Aggregation/Deaggregation of Gold Nanoparticles Induced by a Cleavable Dithiol Linker. *Langmuir* **2005**, *21*, 5537–5541.
26. Sato, K.; Hosokawa, K.; Maeda, M. Rapid Aggregation of Gold Nanoparticles Induced by Non-Cross-Linking DNA Hybridization. *J. Am. Chem. Soc.* **2003**, *125*, 8102–8103.
27. Kendall, M.; Tetley, T. D.; Wigzell, E.; Hutton, B.; Nieuwenhuijsen, M.; Luckham, P. Lung Lining Liquid Modifies Pm(2.5) in Favor of Particle Aggregation: A Protective Mechanism. *Am. J. Physiol. Lung Cell Mol. Physiol.* **2002**, *282*, L109–114.
28. Lundqvist, M.; Stigler, J.; Cedervall, T.; Berggard, T.; Flanagan, M. B.; Lynch, I.; Elia, G.; Dawson, K. The Evolution of the Protein Corona around Nanoparticles: A Test Study. *ACS Nano* **2011**, *5*, 7503–7509.
29. Kreuter, J.; Shamenkov, D.; Petrov, V.; Ramge, P.; Cychutek, K.; Koch-Brandt, C.; Alyautdin, R. Apolipoprotein-Mediated Transport of Nanoparticle-Bound Drugs across the Blood-Brain Barrier. *J. Drug Target* **2002**, *10*, 317–325.
30. Shang, W.; Nuffer, J. H.; Dordick, J. S.; Siegel, R. W. Unfolding of Ribonuclease a on Silica Nanoparticle Surfaces. *Nano Lett.* **2007**, *7*, 1991–1995.
31. Laera, S.; Ceccone, G.; Rossi, F.; Gilliland, D.; Hussain, R.; Siligardi, G.; Calzolai, L. Measuring Protein Structure and Stability of Protein−Nanoparticle Systems with Synchrotron Radiation Circular Dichroism. *Nano Lett.* **2011**, *11*, 4480–4484.